Materials Chemistry and Physics 143 (2014) 838–844

Contents lists available at ScienceDirect

Materials Chemistry and Physics

journal homepage: www.elsevier.com/locate/matchemphys

Covalent functionalization of single-walled carbon nanotubes with anthracene by green chemical approach and their temperature dependent magnetic and electrical conductivity studies

A. Hariharasubramanian [a], Y. Dominic Ravichandran [a,*], R. Rajesh [a], K. Rajendra Kumar [a], M. Kanagaraj [b], S. Arumugam [b]

[a] Organic Chemistry Division, School of Advanced Sciences, VIT University, Vellore 632014, Tamilnadu, India
[b] Centre for High Pressure Research, School of Physics, Bharathidasan University, Thiruchirapalli 620024, India

HIGHLIGHTS

- SWCNTs were functionalized using 2-aminoanthracene by green chemistry.
- Characterized by FTIR, Raman, XRD, SEM and TEM.
- Temperature dependent magnetization and conductivity were investigated.
- 300 fold increase in conductivity was observed for Ant-f-SWCNTs.
- Semiconductor behaviour was observed in the case of Ant-f-SWCNTs.

ARTICLE INFO

Article history:
Received 18 December 2012
Received in revised form
18 September 2013
Accepted 15 October 2013

Keywords:
Magnetic materials
Electrical conductivity
Semiconductors
Hysteresis
Powder diffraction

ABSTRACT

Single-walled carbon nanotubes (SWCNTs) were covalently functionalized with anthracene in molten urea by a green chemical approach. The anthracene functionalized single-walled carbon nanotubes (Ant-f-SWCNTs) were examined along with SWCNTs, using Fourier transform infrared spectroscopy (FTIR), Raman spectroscopy, powder X-Ray diffraction (XRD), and scanning, and transmission electron microscopy. The observations revealed the functionalization of SWCNTs by anthracene. The temperature dependent magnetization (300–5 K) and electrical resistivity were also measured for both SWCNTs and Ant-f-SWCNTs. The electrical resistivity of Ant-f-SWCNTs at 300 K was found to be 1.27 KΩm, which is much lower than 388.55 KΩm for pristine. This indicated a 300 fold increase in conductivity at room temperature for Ant-f-SWCNTs when compared to SWCNTs. The temperature dependence of the conductivity provided an indication of the semiconducting behaviour.

1. Introduction

The one-dimensional (1D) hollow nano structure of single-walled carbon nanotubes (SWCNT) provides a unique model system for coupling with nanometer-sized magnetic objects (small magnetic clusters, metallofullerens, molecular magnets, etc.) by surface functionalization or encapsulation [1]. SWCNTs are ballistically-conducting nanotubes, which are extremely promising class of nano structured materials for diverse applications including magnetic data storage devices, fuel cells, field-emission, scanning microscopy tips [2]. Moreover, SWCNTs provide a unique model for the study of the interactions between magnetic clusters and electron hosts [3]. The major disadvantage is their inability to disperse in organic and inorganic species. The dispersion of carbon nanotubes (CNTs) has thrown open a wide range of applications. Several approaches have already been reported for the dispersion of CNTs in aqueous and organic solvents. Among them, surface functionalization is one of the recent techniques. Functionalization of SWCNTs not only increases the processing durability but also changes their physical and chemical properties [4–8]. Covalent functionalization disrupts the bonding system and breaks the translational symmetry of SWCNTs by the introduction of saturated sp^3 carbon atoms. As a result, electronic and transport properties of SWCNTs are significantly improved [9,10]. One of the methods to study magnetization of the nanotubes is through the use of SQUID magnetometer [11]. Further, under externally applied magnetic

* Corresponding author. Tel.: +91 416 220 2408; fax: +91 416 2243092, +91 416 2245766.
E-mail address: ydominic64@yahoo.co.in (Y. Dominic Ravichandran).

0254-0584/$ – see front matter © 2013 Elsevier B.V. All rights reserved.
http://dx.doi.org/10.1016/j.matchemphys.2013.10.022

field, SWCNTs exhibit paramagnetic or diamagnetic character depending on the chirality of CNTs, Fermi energy level, and the direction of the magnetic field relative to the tube axis [12]. The ferromagnetic behaviour observed in SWCNTs at room temperature extended the applications of functionalized SWCNTs in areas such as magnetic storage media and cell therapies [13,14]. The main objective of our research is the development of useful methods for functionalized SWCNTs with improved magnetic and electrical properties for nanoscale devices [15]. Even though a lot of work has been done on functionalized SWCNTs, the magnetic and electrical properties of functionalized SWCNTs are yet to be studied in detail. Hence, for the first time, we report the preparation of anthracene functionalized SWCNTs (Ant-f-SWCNTs) by an environmentally friendly green chemistry approach and present a study of their magnetic response under externally applied magnetic field using conventional four probe method.

2. Experimental methods

2.1. Materials

SWCNTs were purchased from cheap tubes.com, USA. 2-aminoanthracene was purchased from Sigma Aldrich, India. While Sodium nitrite ($NaNO_2$), urea, sodium hydroxide (NaOH), methanol, *N*,*N*-Dimethylformamide (DMF) and Tetrahydrofuran (THF) were purchased from S.D. fine chemicals, India. All reagents were of analytical grade without further purifications except SWCNTs, which were purified with nitric acid and washed with excess amount of water and methanol.

2.2. Functionalization of SWCNTs

A schematic representation of functionalization of SWCNTs with 2-aminoanthracene is depicted in Fig. 1. The environment friendly functionalization of SWCNTs using molten urea as solvent was carried out, as demonstrated earlier by Tour et al. [16]. This protocol is superior to other methods because of the involvement of lesser reaction time.50 mg of SWCNTs were added to the mechanically stirred molten urea at 145 °C, and the mixture was homogenized for 5 min. Then, 200 mg of 2-aminoanthracene was added to the above reaction mixture, and stirred for 5 min. Finally, to the above mixture, 276 mg solid sodium nitrite was added slowly, where a rapid N_2 gas evaluation was observed. Further stirring was continued for 5 min. Then the reaction mixture was poured into an Erlenmeyer flask containing 200 ml of double distilled water. The functionalized SWCNTs were washed several times with hot distilled water followed by methanol and THF. The dispersed Ant-f-SWCNTs were centrifuged and dried in a hot air oven for about 24 h. Ant-f-SWCNTs have excellent dispersibility in organic solvents (as shown in Fig. 2) such as DMF and THF.

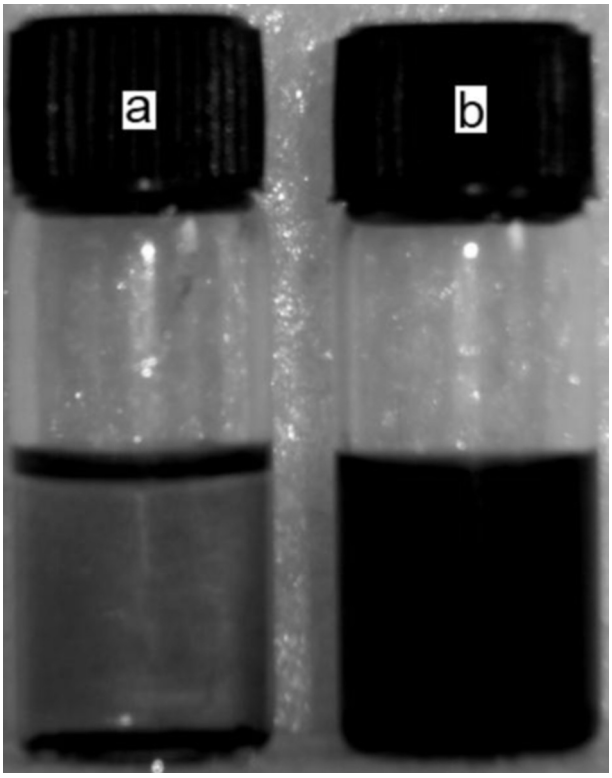

Fig. 2. Dispersion of (a) SWCNTs (b) Ant-f-SWCNTs in DMF.

2.3. Characterization techniques

Surface modification of SWCNTs was checked using Fourier transform infrared spectroscopy (FTIR) in Perkin–Elmer Spectrum-1 instrument with freshly dried KBr pellets in the range of 4000–400 cm^{-1}. Raman spectra was recorded using Jobin yvon HR800UV Raman spectrometer equipped with 633 nm He–Ne laser in the range of 2000–200 cm^{-1}. Powder X-ray diffraction (XRD) measurements were recorded with D8 advance Bruker AXS diffractometer using CuKα radiation ($\lambda = 1.5406$ Å). Alumina was used as a standard to eliminate instrument peak broadening. The morphology of the samples was evaluated using field emission-

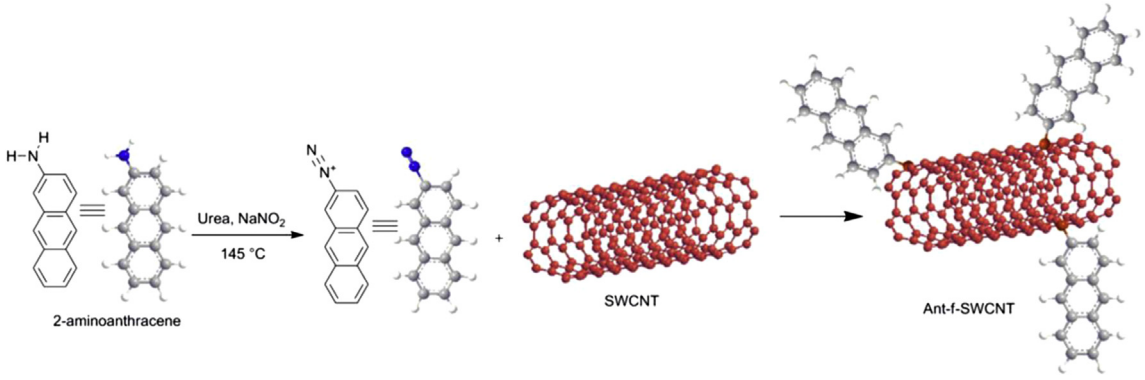

Fig. 1. Anthracene functionalization of SWCNTs.

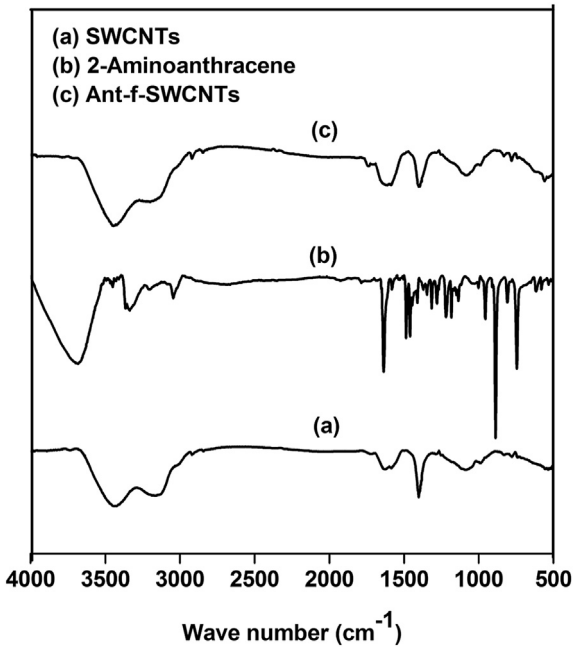

Fig. 3. FTIR spectra (a) SWCNTs (b) 2-aminoanthrancene (c) Ant-f-SWCNTs.

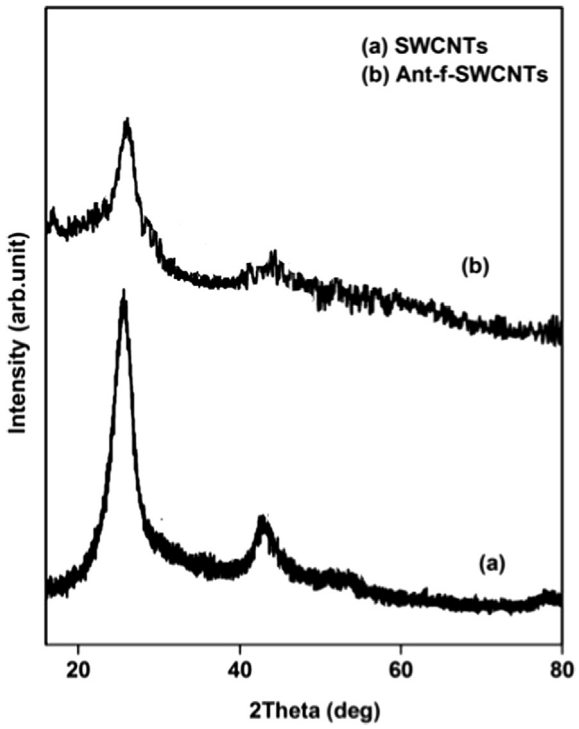

Fig. 5. XRD pattern for (a) SWCNTs (b) Ant-f-SWCNTs.

scanning electron microscopy (FE-SEM) (JSM-6700, JEOL, Japan). The particle size and the morphology of the sample were observed by a transmission electron microscopy (TEM) instrument operating at 200 KV (JEM 2010-JEOL ltd, Japan). Magnetic studies were carried out using 9 T physical property measurement system (PPMS) – vibrating sample magnetometer module (Quantum design, USA). Electrical resistivity measurement for the samples was carried out after pelletizing them using hydraulic pressure-Riken, Japan with 7.5 MPa pressure. The pelletized samples were kept in a hot air oven at 100 °C for about an hour to remove any moisture. The temperature dependent electrical resistivity of the samples was measured by conventional four probe technique, using a closed cycle He-cryostat (Closed cycle refrigerator system – variable temperatures insert (4–800 K) (Sumitomo, Japan). A programmable current source (2 mA) was used for applying constant current, and the resulting voltage was measured with a programmable voltmeter.

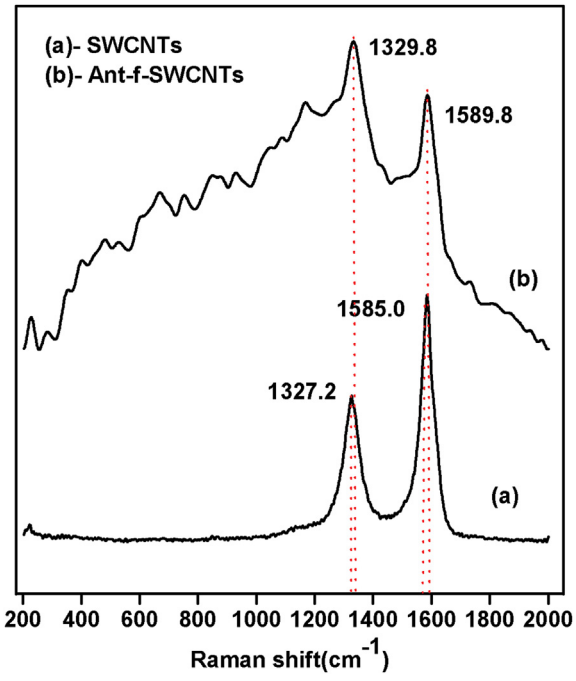

Fig. 4. Raman spectra (a) SWCNTs (b) Ant-f-SWCNTs.

3. Results and discussion

Ant-f-SWCNTs were characterized using powerful tools including FTIR, Raman spectroscopy, and XRD to elucidate the covalent functionalization. The FTIR spectra of SWCNTs, anthracene and Ant-f-SWCNTs are shown in Fig. 3(a)–(c) respectively. Peaks were observed around 3400, 1630, 1402 and 1215 cm^{-1} for both SWCNTs and Ant-f-SWCNTs due to the –OH and COOH functionalities [17]. The C–H stretching frequencies due to carbon network of nanotubes were observed near 2950 cm^{-1} for SWCNTs, whereas in the case of Ant-f-SWCNTs, the peak got sharpened further due to the contribution of anthracene moiety [18]. Further, the appearance of additional peaks in Ant-f-SWCNTs spectra at 3019, 1525 and 769 cm^{-1} occurred due to the aromatic C–H stretching, C–C bond stretching and C–H out of plane bending mode respectively. The above observations confirmed the covalent functionalization of anthracene molecule on the sidewalls [19,20].

Further, the Raman spectra also furnished a clear evidence for the covalent functionalization of SWCNTs. In Raman spectra, SWCNTs exhibited two characteristic peaks at 1585 cm^{-1} and 1327 cm^{-1}. The G-band (Tangential mode) appeared at 1585 cm^{-1}. This could be attributed to the Raman active optical phonon mode E_{2g} of 2D graphene. The origin of the peak at 1327 cm^{-1} might be due to the disorder induced D-band, and its appearance can be assigned to the symmetry lowering effect due to the introduction of defects and attachment of different chemical species [21]. For Ant-f-SWCNTs, the G and D-bands appeared with slight deviation at

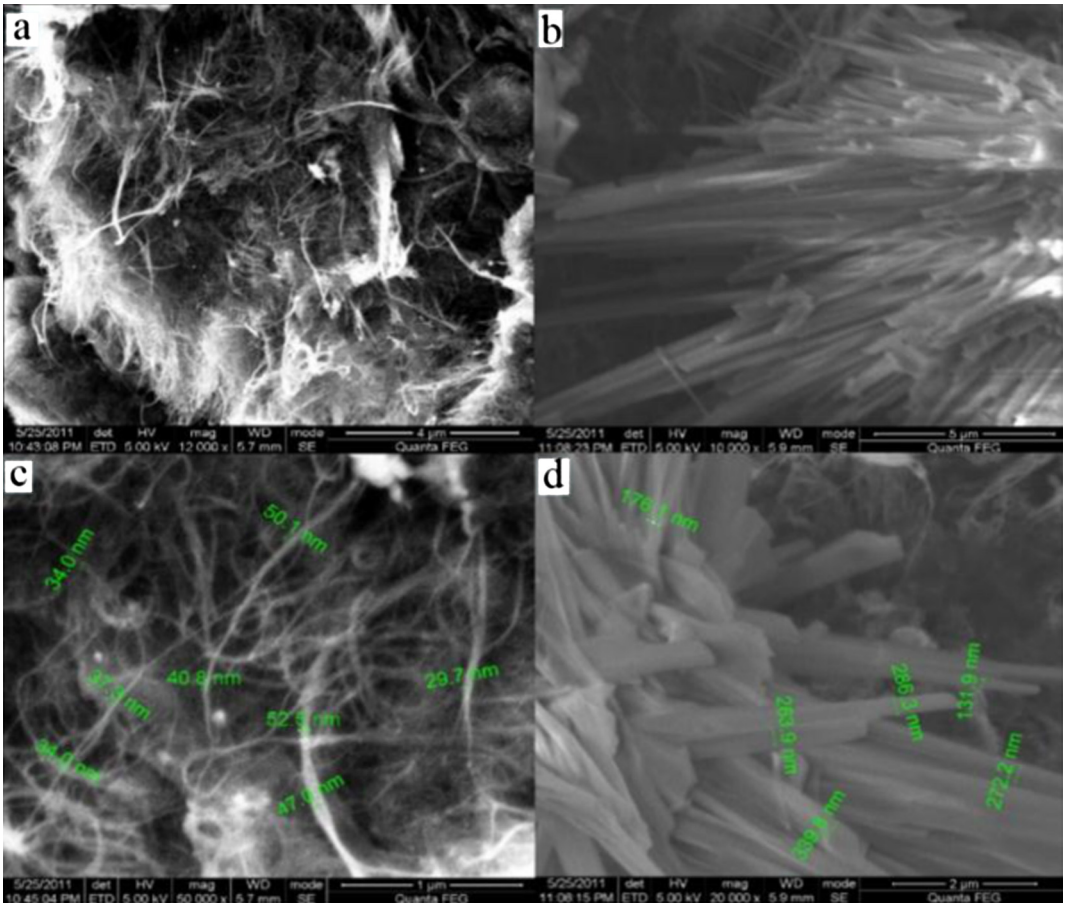

Fig. 6. SEM images (a and c) SWCNTs (b and d) Ant-f-SWCNTs.

1589 and 1329 cm^{-1} respectively. These deviations might have been due to the charge transfer processes between SWCNTs and anthracene molecules [22]. Further, the increase in intensity of D-band for Ant-f-SWCNTs, when compared to SWCNTs, could be due to the introduction of sp^3 carbon atoms onto the SWCNTs [23,24]. Furthermore, the enhanced intensity ratio I_D/I_G for Ant-f-SWCNTs (1.04), compared to SWCNTs (0.66), may be due to the contribution of sp^3 hybridized carbon atom from anthracene [25]. These observations added evidence to the functionalization of anthracene on the SWCNTs (Fig 4).

Fig. 5 represents the XRD studies of SWCNTs and Ant-f-SWCNTs. The graphitic carbon of SWCNTs exhibited diffracted peak at 25.6° (2θ) where as the Ant-f-SWCNTs showed a higher value of 2θ at 26.2°. This shift could be due to the functionalization of SWCNTs. The average interplanar distance (d) and the average crystalline size were calculated using Bragg's law. The average interplanar distance was found to be 3.48 Å and 3.45 Å for SWCNTs and Ant-f-SWCNTs respectively. Further, the average crystalline size for SWCNTs and Ant-f-SWCNTs was calculated to be 25.58 nm and 27.54 nm respectively. The changes in 2θ values and average d-spacing value confirmed the crystallographic rearrangements in the Ant-f-SWCNTs [26].

Electron microscopic observations were performed to envisage the structural aspects and morphology of the prepared Ant-f-SWCNTs. FE-SEM images of the SWCNTs and the Ant-f-SWCNTs are shown in Fig. 6(a)–(d). FE-SEM images showed that Ant-f-SWCNTs are bundled together, and tubes are less isolated and distinct as compared to that of the SWCNTs. The bundling of nanotubes in Ant-f-SWCNTs is due to the enhanced van der Waals interactions among the tubes. From Fig. 6(a)–(d) it is also evident that the tubular structures of SWCNTs were intact even after functionalization [27]. Furthermore, the covalent functionalization of SWCNTs considerably increased the diameter of the SWCNTs, which could be clearly visualized, and these observations proved to be strong evidences for the covalent functionalization of anthracene.

To authentically confirm the covalent functionalization of SWCNTs, the TEM images were recorded. The TEM images, given in Fig. 7, confirm the morphology and the nano structure of Ant-f-SWCNTs. TEM images reveal a spaghetti-like morphology Fig. 7(a) and (c) for SWCNTs. While the Ant-f-SWCNTs had coaxially tubular structure, and its walls were well encapsulated with the anthracene moiety (Fig. 7(c)), the diameter of the Ant-f-SWCNTs was found to be around 10 nm with single graphitic layer as indicated in the image Fig. 7(d). The core shell structure clearly indicated the covalent links between the anthracene and the SWCNTs. Further, the TEM studies throw light on the dispersion of Ant-f-SWCNTs.

3.1. Magnetic property measurement

Fig. 8 shows the plot of temperature dependence of magnetization (M) for SWCNTs and Ant-f-SWCNTs with an applied magnetic field of 0.1 T. It is clear that the observed magnetization property of SWCNTs and Ant-f-SWCNTs completely depends on the temperature. At room temperature, SWCNTs had higher magnetization value than that of functionalized one. The value of M for SWCNTs was 0.258 $Am^2\ g^{-1}$ and for Ant-f-SWCNTs 0.203 $Am^2\ g^{-1}$ at 300 K. As temperature decreases, the magnetization value for

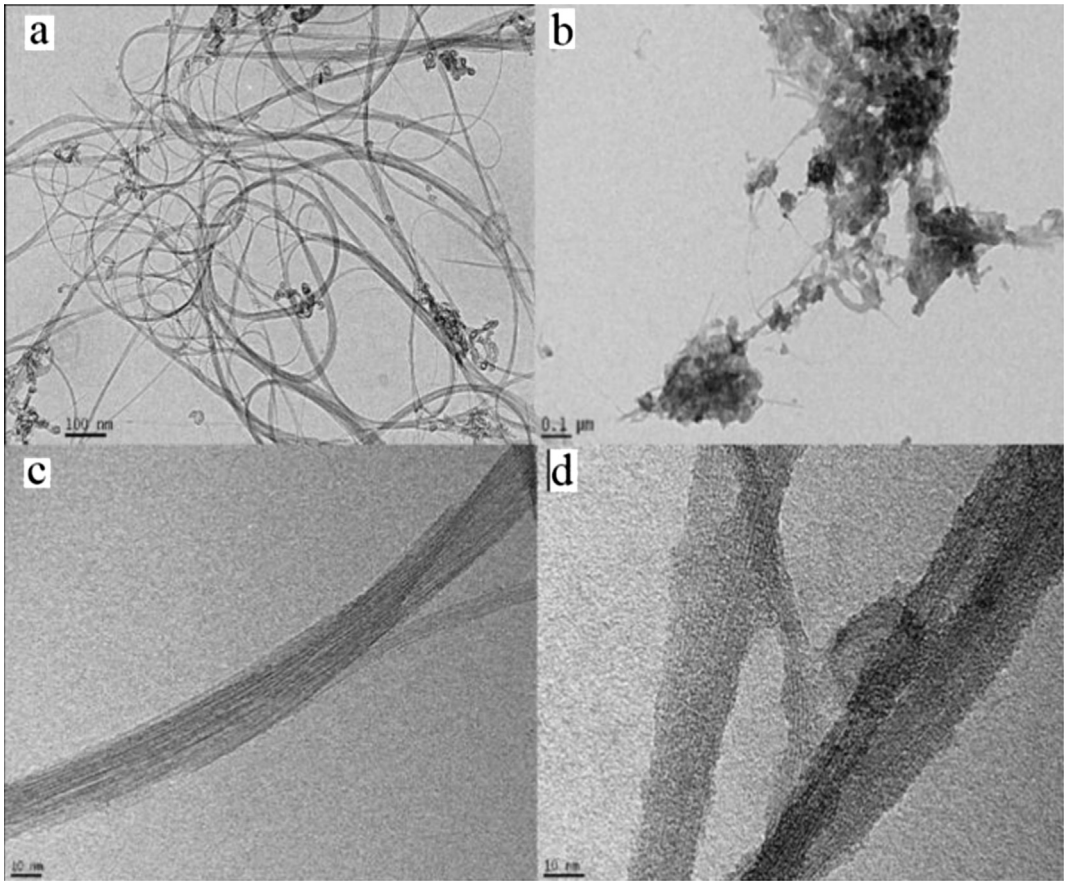

Fig. 7. TEM images (a and c) SWCNTs (b and d) Ant-f-SWCNTs.

both SWCNTs and Ant-f-SWCNTs increases. A sudden increase of magnetization was noted below 85 K where the *M* value of Ant-f-SWCNTs was slightly higher than that of SWCNTs. The rise in temperature leads to increase in the magnitude of thermal vibration of a material which in turn extends to randomization of the direction of spin magnetic moments that could be aligned. This could be the reason, that at low temperature, the alignment of domains in the directions of applied magnetic field for the functionalized SWCNTs was more because of the extended covalently attached aromatic system.

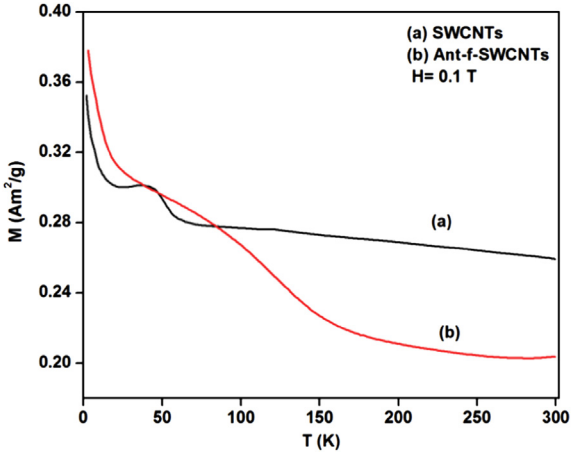

Fig. 8. *M* vs. *T* curve for SWCNTs and Ant-f-SWCNTs.

Pure SWCNTs are diamagnetic in character. Previous reports gave the magnetization value for SWCNTs encapsulated with iron nanoparticles as 2.6 $Am^2\ kg^{-1}$ at 5 K. In this case, the magnetization of SWCNTs was observed to be 0.328 $Am^2\ g^{-1}$ at 5 K. If iron nanoparticles were encapsulated in SWCNTs the value would be around 2.6 $Am^2\ kg^{-1}$ at 5 K, whereas we observed the magnetization value of 0.328 $Am^2\ kg^{-1}$ for the Ant-f-SWCNTs at 5 K. The lower magnetization value may be because of the lower percentage of functionalization. This provides affirmative evidence for the ferromagnetic property of SWCNTs due to functionalization of SWCNTs with anthracene, and is not because of the presence of iron nanoparticles [28]. For SWCNTs, the value of magnetization changed from 0.258 $Am^2\ g^{-1}$ at 300 K to 0.328 $Am^2\ g^{-1}$ at 5 K, while for the covalently functionalized Ant-f-SWCNTs it increased from 0.203 $Am^2\ g^{-1}$ at 300 K to 0.364 $Am^2\ g^{-1}$ at 5 K.

Fig. 9 shows the plots of Magnetization (*M*) versus external applied magnetic field up to ±3 T for SWCNTs and Ant-f-SWCNTs, which were measured at five consecutive temperatures (300, 250, 150, 50, 35, and 5 K). Clear hysteresis loops were observed at 5 and 300 K for the samples, as depicted in Fig. 10. The discrepancy between hysteresis curves in Fig. 10(a) and (b) might be due to randomization of the Fe nanoparticles causing its spin canting effect, which arises under high externally applied magnetic field. It was clearly observed that the values of saturation magnetization (M_s), Remenance (M_r) and Coercivity (H_c) increased with the decrease of temperature. The coercivity values calculated from Fig. 10 for both SWCNTs and Ant-f-SWCNTs at 300 K and 5 K were higher than that of bulk Fe ($H_c = 0.9\ O_e$) [29]. This clearly indicates that covalently functionalized SWCNTs have higher magnetic stability due to the functionalization of anthracene [30].

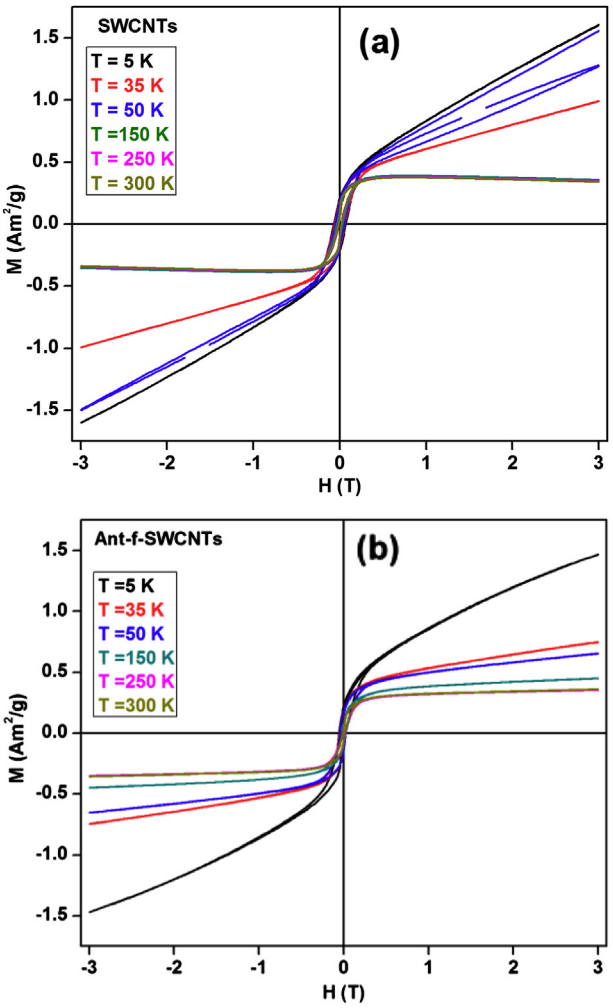

Fig. 9. Hysteresis loops for (a) SWCNTs and (b) Ant-f-SWCNTs at various temperatures (from 300 K to 5 K) and applied magnetic field of about ±3 T.

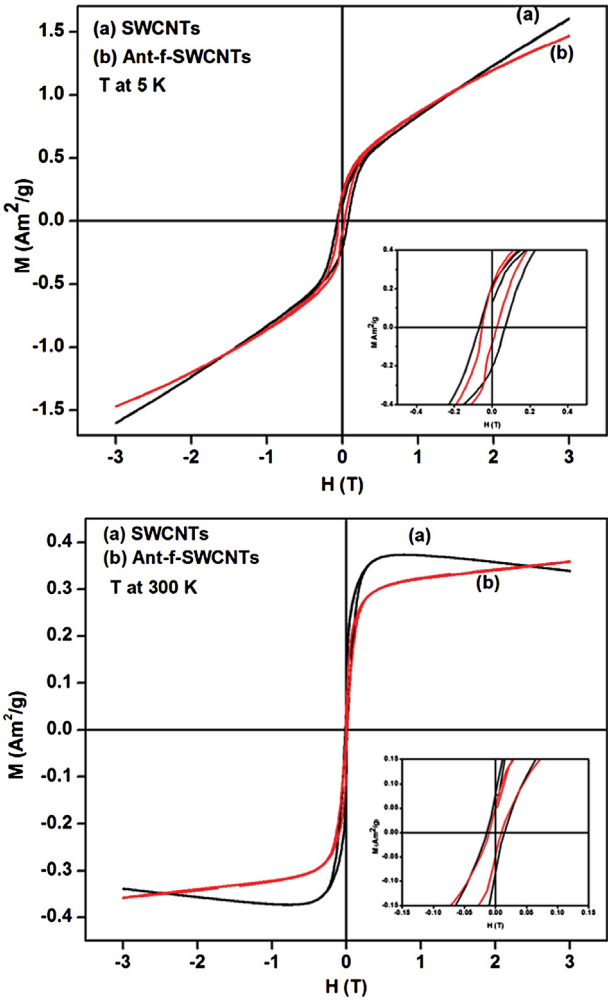

Fig. 10. Hysteresis loops for SWCNTs and Ant-f-SWCNTs at 5 and 300 K respectively under the magnetic field ±3 T. The right insert shows the magnification area of the hysteresis loop.

3.2. Electrical resistivity measurement

The temperature dependent dc-resistivity of SWCNTs and Ant-f-SWCNTs is depicted in Fig. 11. The Functionalized SWCNTs find diverse applications in areas such as nanometer sized semiconductor devices and inter-connectors. Studies on the electrical transport properties of functionalized SWCNTs are vital in order to realize their applicability towards newer electronic devices. To find the conducting properties of SWCNTs and Ant-f-SWCNTs, dc resistivity as a function of temperature was measured using the conventional four probe method. From Fig. 11, it is clearly observed that the anthracene functionalization really caused dramatic change in the electrical transport property of SWCNTs. For Ant-f-SWCNTs, the value of resistivity at 300 K was found to be 1.27 KΩm, which is much lower when compared with the values of SWCNTs 388.55 KΩm observed at that temperature. This is an indication of the semiconducting behaviour between 300 K and 2 K. The resistivity measured for Ant-f-SWCNTs was 1.27 KΩm at 300 K which is much lower compared to the values of SWCNTs 388.55 KΩm. This clearly indicated that functionalization by anthracene in SWCNTs showed peculiar enhancement of conductivity in the range of 300 to 5 K. The π-π electron interaction between anthracene moiety and the SWCNTs increases the conductive nature of Ant-f-SWCNTs [31].

4. Conclusion

Covalent functionalization of the SWCNTs with amino-anthracene profoundly changed the magnetic response and

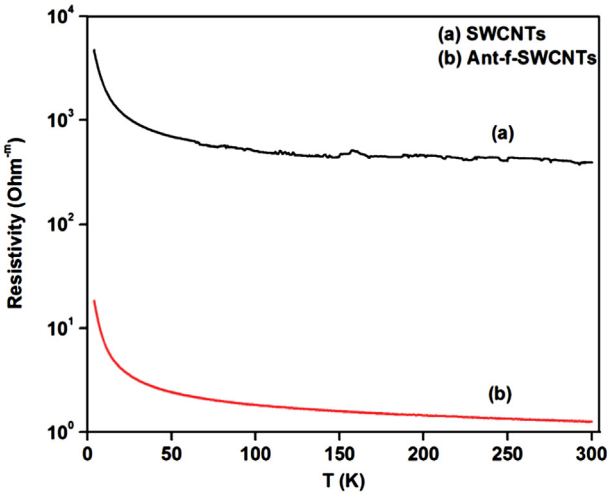

Fig. 11. Electrical resistivity vs *T* of SWCNTs and Ant-f-SWCNTs.

electrical conductivity of this system. It can be understood that the relative dimensions of the core and the shell determine not only the coercivity and exchange field but also the dominant reversal mechanism of the Ant-f-SWCNTs component. This is the first time demonstration of the temperature dependent magnetization and hysteresis studies of SWCNTs and Ant-f-SWCNTs. Four-probe measurements indicated a 300 fold increase in conductivity at room temperature for Ant-f-SWCNTs when compared to SWCNTs. The temperature dependence of the conductivity gave a good indication of the semiconducting behaviour, which implies the extended conjugated sp^2 network in Ant-f-SWCNTs. These findings validate Ant-f-SWCNTs as potential candidates for future high performance electronics [32–35].

Acknowledgements

The support and encouragement from the management of VIT University, Vellore is greatly acknowledged. In addition the authors also thank SAIF, School of Advanced Sciences jointly funded by VIT University, Vellore and DST-FIST and SAIF-IITM for the spectral analysis. Further, the authors thank DST and UGC for the financial support of PPMS at Center for High Pressure Research, School of Physics, Bharathidasan University. Prof. R. Srinivasan, Assistant Director, International Relations, VIT University is greatly acknowledged for the proof correction.

References

[1] N. Roch, S. Florens, V. Bouchiat, W. Wersndorfer, F. Balestro, Nature 453 (2008) 633–637.
[2] S. Liu, Q. Shen, Y. Cao, L. Gan, Z. Wang, M.L. Steigerwald, X. Guo, Coord. Chem. Rev. 254 (2010) 1101–1106.
[3] M. Ouyang, J. Huang, C.M. Lieber, Acc. Chem. Res. 35 (2002) 1018–1025.
[4] P. Singh, S. Campidelli, S. Giordani, D. Bonifazi, A. Bianco, M. Prat, Chem. Soc. Rev. 38 (2009) 2214–2220.
[5] J. Zhao, H. Park, J. Han, J.P. Lu, J. Phys. Chem. B 108 (2004) 4227–4230.
[6] M.L. Tang, J.H. Oh, A.D. Reichardt, Z. Bao, J. Am. Chem. Soc. 131 (2009) 3733–3740.
[7] N.A. Kumar, I.Y. Jeon, G.J. Sohn, R. Jain, S. Kumar, J.B. Baek, ACS Nano 5 (2011) 2324–2331.
[8] C.F. Chiu, N. Dementev, E.J. Borguet, Phys. Chem. A 115 (2011) 9579–9584.
[9] N. Karousis, N. Tagmatarchis, D. Tasis, Chem. Rev. 110 (2010) 5366–5397.
[10] M. Zaka, Y. Ito, H. Wang, W. Yan, A. Robertson, Y.A. Wu, M.H. Rummeli, D. Staunton, T. Hashimoto, J.J.L. Morton, A. Ardavan, G.A.D. Briggs, J.H. Warner, ACS Nano 4 (2010) 7708–7716.
[11] V. Ellis, B. Ingham, J. Magn. Magn. Mater. 302 (2006) 378–381.
[12] M. Kibalchenko, M.C. Payne, J.R. Yates, ACS Nano 5 (2011) 537–545.
[13] S. Park, M. Cha, J. Lee, Diamond Relat. Mater. 19 (2010) 942–945.
[14] E. Borowiak-Palen, E. Mendoza, A. Bachmatiuk, M.H. Rummeli, T. Gemming, J. Nogues, V. Skumryev, R.J. Kalenczuk, T. Pichler, S.R.P. Silva, Chem. Phys. Lett. 412 (2006) 129–133.
[15] Y. Shinya, Y. Murata, K. Kubo, K. Tomita, K. Motoyoshi, T. Kimura, H. Okino, R. Hobara, I. Matsuda, S.I. Honda, M. Katayama, S. Hasegawa, Nano. Lett. 7 (2007) 956–959.
[16] C.D. Doyle, J.M. Tour, Carbon 47 (2009) 3215–3218.
[17] H. Kitamura, M. Sekido, H. Takeuchi, M. Ohno, Carbon 49 (2011) 3851–3856.
[18] R. Tian, X. Wanga, M. Li, H. Hua, R. Chen, F. Liu, H. Zheng, L. Wan, Appl. Surf. Sci. 255 (2008) 3294–3299.
[19] G. Gabriel, G. Sauthier, J. Fraxedas, M.M. Manas, M.T. Martinez, C. Miravitlles, J. Casabo, Carbon 44 (2006) 1891–1897.
[20] F. Buffa, H. Hu, D.E. Resasco, Macromolecules 38 (2005) 8258–8263.
[21] Z. Liu, J. Zhang, B. Gao, Chem. Commun. (2009) 6902–6918.
[22] Y. Ouyang, L.M. Cong, L. Chen, Q.X. Liu, Y. Fang, Physica E 40 (2008) 2386–2389.
[23] B. Gebhardt, A. Hirsch, Z. Syrgiannis, C. Backes, R. Graupner, F. Hauke, J. Am. Chem. Soc. 133 (2011) 7985–7995.
[24] M.S. Dresselhaus, G. Dresselhaus, R. Saito, A. Jorio, Phys. Rep. 409 (2005) 47–99.
[25] W. Chidawanyika, T. Nyokong, Carbon 48 (2010) 2831–2838.
[26] A.M. Shanmugharaj, J.H. Bae, K.Y. Lee, W.H. Noh, S.H. Lee, S.H. Ryu, Compos. Sci. Technol. 67 (2007) 1813–1822.
[27] D.K. Singh, P.K. Iyer, P.K. Giri, Nanotrends J. Nanotechnol. Appl. 4 (2008) 55–58.
[28] Y. Li, T. Kaneko, T. Ogawa, M. Takahashi, R. Hatakeyama, Jap. J. Appl. Phys. 47 (2008) 2048–2055.
[29] F. Geng, H. Cong, Physica B 382 (2006) 300–304.
[30] M. Ritschel, D. Elefant, N. Mattern, K. Biedermann, S. Hampel, Ch. Muller, T. Gemming, B. Buchner, J. Appl. Phys. 98 (1–5) (2005) 074315.
[31] O.K. Park, T. Jeevananda, N.H. Kim, S. Kim, J.H. Lee, Scripta. Mater. 60 (2009) 551–554.
[32] A. Javey, H. Kim, M. Brink, Q. Wang, A. Ural, J. Guo, P. McEuen, M. Lundstrom, H. Dai, Nat. Mater. 1 (2002) 241–246.
[33] A. Javey, J. Guo, Q. Wang, M. Lundstrom, H. Dai, Nature 424 (2003) 654–657.
[34] P.L. McEuen, M.S. Fuhrer, H.K. Park, IEEE Trans. Nanotechnol. 1 (2003) 78–85.
[35] S. Wind, J. Appenzeller, R. Martel, V. Derycke, P.H. Avouris, Appl. Phys. Lett. 80 (2002) 3817–3819.